

Supporting Information

Bridging Dynamics of Telechelic Polymers between Solid Surfaces

Hossein Rezvantalab and Ronald G. Larson*

*Department of Chemical Engineering, University of Michigan, Ann Arbor, Michigan,
48109, USA*

**Corresponding author, Email: rlarson@umich.edu*

Effect of solid surfaces on the first-passage time of polymers. As mentioned in the main text, the analysis of Cao, Likhtman and coworkers³⁰ deals with the first-passage problem for Rouse chains in the bulk. For the present bridging problem where the polymer is bounded between solid surfaces representing colloidal particles, the first-passage time to reach a given distance is affected by the repulsion of polymer beads from the surfaces. For polymer chains with one end fixed at the origin $z=0$, the presence of a solid surface at $z=0$ is expected to reduce the first-passage time, τ_f , due to restricted motion in the $-z$ direction. Note that in our analysis, we do not consider the opposite surface placed at $z = d$ and the associated repulsive potential since the internal beads rarely cross the location of that surface for the considered gaps larger than the polymer's equilibrium length. To evaluate the effect of the solid surface on the first-passage time, we perform FFS simulations on polymer chains without end stickers in the bulk, and compare the first-passage time derived from these FFS simulations that lack the solid

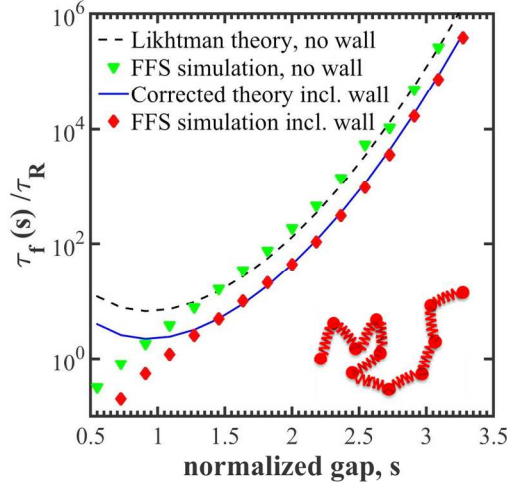


Figure S1. The first-passage time for loop-to-bridge transition for 10-spring Rouse polymers without end stickers as a function of the normalized extension with and without the effect of the wall, compared with Likhtman's original theory for those two cases, showing that the presence of the wall speeds the transition three-fold, consistent with corrected expression, Eq. (17).

surface with that obtained from FFS simulations in presence of the surface. Note that the starting conformation for the polymer chain in the bulk corresponds to both fixed and free ends at $z=0$ to resemble the loop conformation of the chain next to the surface. The first-passage time normalized by the polymer relaxation time is shown in Figure S1 for a Rouse chain with $N_K = 100$ Kuhn steps and $N = 10$ springs. We note that in the absence of the wall, the simulation result for $s > 1.5$ is in very good agreement with Likhtman's original expression³⁰ for a one-dimensional Rouse chain in the bulk. However, adding the solid surface results in ~ 3 -fold reduction in the first-passage time for all normalized gaps. We verified a similar scaling for polymers of different root-mean-square end-to-end distances and different number of springs. Therefore, an empirical factor $1/3$ is introduced in Eqs. (14) and (17) to take into account the correction due to presence of the solid surface at $z=0$.

Effect of excluded volume potential between polymer beads on the first-passage time. The excluded volume potential between the beads in a realistic polymer chain also influences the first-passage time. While an analytical expression such as the one given by Eq. (17) cannot be readily developed, BD simulations can be used for the range of chains lengths and extensions that are computationally accessible. As an example, we show in Figure S2 the effect of adding a 6-12 LJ potential with $\sigma = 1.3[b_K]$ and $\varepsilon = 1.3[k_B T]$ to a Rouse chain with $N_K = 100$ Kuhn steps and $N = 10$ springs. The parameters are selected so that the end-to-end distance distribution and radius of gyration match those of the PEO300 molecule at dry Martini level.³² We note from Figure S2(a) that the excluded volume interaction does not change the scaling of the first-passage time with normalized gap and produces only a modest deviation from the first passage time for the chain without the excluded volume interaction (Note that the relaxation time, τ_R , used for normalizing the result in both cases is the Rouse time without including the excluded volume effects). Renormalizing the first-passage times by $\exp(3s^2/2)/s$ in Figure S2(b) better demonstrates the variation: the excluded volume potential between the beads reduces the first-passage for $s > 1.5$ up to 40%, while the asymptotic behavior is preserved. This suggests that one could possibly use the generalized form given by Eq. (14) and fit the functions $C_1(N)$ and $C_2(N)$ for the Rouse chain including excluded volume effects. Such an expression would, however, depend on the particular shape of the added potential and selected well depth/range, which is generally a function of the molecular weight of the polymer.

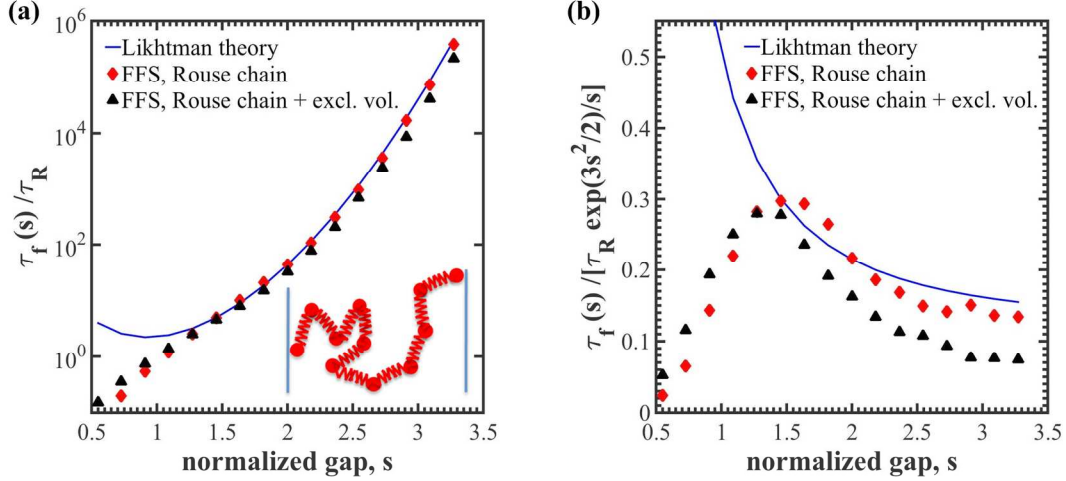


Figure S2. The effect of excluded volume potential between the beads using a 6-12 LJ excluded volume potential with $\sigma = 1.3[b_K]$ and $\varepsilon = 1.3[k_B T]$ on first-passage time for loop-to-bridge transition for 10-spring Rouse chains without end stickers as a function of the normalized gap between the surfaces, in comparison with the theoretical expression given by Eq. (17).

Mapping the FJC model onto a Rouse chain. The loop-to-bridge transition time for the finer-grained representation of the polymer using the freely-jointed chain (FJC) model with $N_K = 100$ Kuhn steps where each spring corresponds to a single Kuhn step was mapped onto that of a Rouse chain with similar root-mean-square end-to-end distance and $N = 5$ springs in the main text. This suggests that 100 constrained modes in the FJC model with $N_K = 100$ is approximately equivalent to $N_K/20 = 5$ effective Rouse modes. We checked the universality of this mapping for polymer chains of different lengths. The first-passage times normalized by $\tau_R \exp(3s^2/2)/s$ are shown in Figure S3 for FJC polymers with two other lengths, namely $N_K = 50$ and 150 Kuhn steps in comparison with those from Eq. (17) for Rouse chains with similar equilibrium length represented by different numbers of springs. We observe that at sufficiently large extensions where both FFS and theory are reliable, the freely-jointed representation approaches the Rouse chain prediction with $N \approx N_K/20 = 2.5$ and 7.5, respectively. Note that for longer polymer

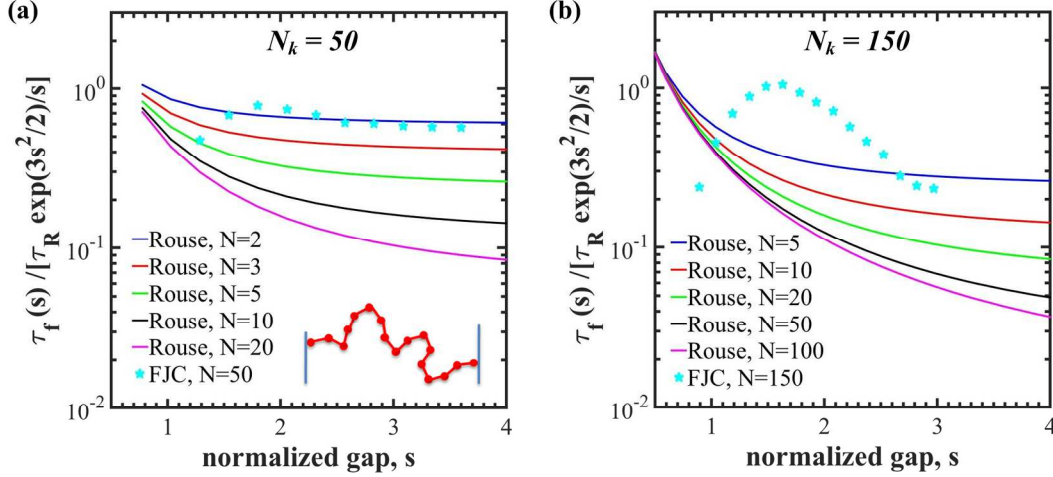


Figure S3. Universality of the FJC-to-Rouse mapping for different polymer chain lengths: the first-passage time for loop-to-bridge transition renormalized by $\tau_R \exp(3s^2/2)/s$ as a function of the normalized gap for polymer chains with no sticker represented by different numbers of Hookean (*i.e.*, Rouse) springs in comparison with a freely-jointed chain (FJC) model of similar equilibrium length for (a) $N_K = 50$, and (b) $N_K = 150$ Kuhn steps. The symbols are from FFS simulations and the solid lines are predictions of Eq. (17) for different numbers of springs.

chains, the asymptotic region where excellent agreement is obtained between the Rouse theory and FFS data for FJC shifts to larger normalized gaps. Moreover, for short polymers with $N_K < 20$, the considered range of normalized extensions $1.5 < s < 4$ corresponds to the chain approaching its fully-extended length, so that the mapping onto a Rouse model breaks down. Such short polymers are, however, irrelevant in most practical applications, so that using Eqs. (17, 19) with $N = N_K/20$ is expected to give a reasonable estimate of the loop-to-bridge transition time for realistic polymer chains between colloids/surfaces.

Relaxation time of model chain. From the Rouse model, the longest stress relaxation time (which is twice the Rouse rotational relaxation time τ_R discussed in the main text) of a multiple-bead chain is $\tau_{Rouse} = \frac{6[\eta]M_w\eta_s}{\pi^2 N_A k_B T}$, where $\eta_s = 8.90 \times 10^{-3}$ dyn·s/cm³ is the solvent viscosity taken to be that of water at 25°C; M_w is the polymer molecular weight;

N_A is Avogadro's number; and $[\eta] = KM_w^\nu$ is the intrinsic viscosity of the polymer, controlled by two empirical constants, which for polyethylene oxide (PEO) are $K = 0.00875 \text{ cm}^3/\text{g}$ and $\nu = 0.79$.^{S1} For PEO, a Kuhn segment contains roughly 3 monomers comprising a molecular weight of 137g/mol.^{S2} A PEO chain with $N_K = 100$ Kuhn steps, therefore corresponds to a molecular weight M_w of 13,700. From these, we get $\tau_{Rouse} = 48.5 \text{ ns}$.

On the other hand, considering a model Rouse chain with N_K Kuhn steps at the dumbbell level, the stress relaxation time can be expressed as $\zeta_i/4H$, where ζ_i is the bead friction coefficient and $H = 3[k_B T]/(N_K[b_K]^2)$ is the spring constant. With $\zeta_i = 100[m]/[t]$ and the energy, mass, and length scales set to unity in LAMMPS units, and eliminating the unit of mass $[m]$ using $[m] = [k_B T][t]^2/[b_K]^2$, the relaxation time of a simulated chain with $N_K = 100$ Kuhn steps is obtained as $(10^4/12)[t] = 833.3[t]$. Equating this to the experimental relaxation time $\tau_{Rouse} = 48.5 \text{ ns}$ yields a unit time of $[t] = 58.2 \text{ ps}$ for this sample chain corresponding to a molecular weight M_w of 13,700.

Thermodynamics of bridge-loop equilibrium. Apart from the dynamics of loop-to-bridge and bridge-to-loop formation, we also evaluate the fraction of each species at equilibrium. Direct BD simulations are performed on Rouse chains with $N_K = 100$ Kuhn steps and $b_K = 1$ represented by different numbers of springs. The polymer chains have end stickers with adsorption free energy $\varepsilon = 8[k_B T]$, and all other simulation parameters are as specified in the main text. A dilute solution of polymers is placed between solid surfaces at different gaps and the fraction of bridging species at equilibrium is calculated. The simulation result is compared with Bhatia and Russel's theoretical analysis for

telechelic associative polymers between flat plates.^{S3} Note that in their theory, there is a missing integral in Eqs. (14) so that the normalized segment density of the chains starting on the right wall and ending on the left wall is not accounted for using mirror subchain expressions to those in their Eq. (14b). A consequence of this error is that a bridge fraction of $1/3$ is obtained at equilibrium rather than $1/2$, which is not reasonable noting that with negligible stretching energy at small gaps, each end sticker would have equal probability of being on surface A or surface B. As such, the two stickers would have a probability of $1/4$ to be both located on surface A, a probability of $1/4$ to be both located on surface B, and a combined probability of $1/2$ to be located on opposite surfaces yielding a bridge. We thus correct their theory by accounting for the missing integral in segment density expressions, which recovers the expected equilibrium distribution of half bridges and half loops at small gaps. Our BD simulation result is compared with the original and corrected theoretical solution in Figure S4. Note that the bridge fraction at close separations approaches $1/2$ irrespective of the number of springs used in polymer chain representation, which is consistent with the corrected theory. At larger gaps, the agreement with theory improves with increasing numbers of springs up to 20, as the refinement in the discrete Rouse chain allows better representation of a continuous Gaussian chain. The agreement observed in the equilibrium distribution of species between our simulations and the available theoretical solution at multiple gaps is another step towards validating the methodology employed here for modeling the polymer-colloid system.

Furthermore, both the theory and BD simulations suggest that the fraction of bridges drops below 5% when the normalized gap becomes larger than 2, and since the fraction

decays exponentially with normalized gap, it should be less than 2% for dimensionless gaps of 3 or more. Note that we are normalizing the gap d with the root-mean-square end-to-end distance of the polymer chain, $N_K^{1/2} b_K$, to be consistent with the notation given for s in the main text. With $N_K = 100$ and $b_K = 1$, the extension beyond which the bridge fraction is less than 2% corresponds to 30% of the fully-extended chain length, $N_K b_K$. We verified that such a limit holds for polymer chains of different length, so our rate analysis would be relevant for such relatively low extensions where a reasonable portion of polymer species form bridges between the surfaces at equilibrium. As discussed in the text, for higher sticker energies, our analysis should be valid for even larger chain extensions, where the bridge fraction is even smaller than 2%.

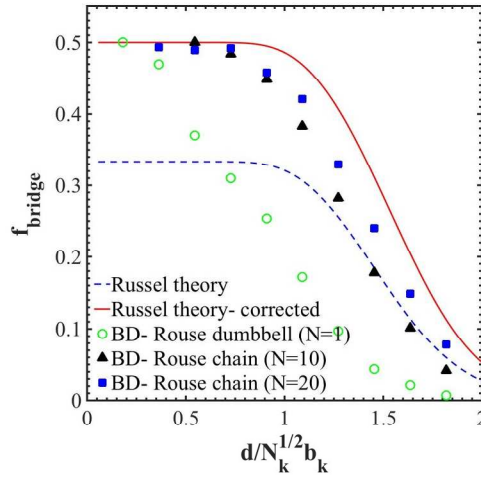


Figure S4. Equilibrium fraction of bridging species in a dilute solution of polymers as a function of the gap between solid surfaces normalized by root-mean-square end-to-end distance. The symbols are from direct BD simulations, where the polymer is represented as a Rouse chain comprised of 1, 5, 10, and 20 springs, and the two end beads stick to the surfaces with an adsorption energy of $\varepsilon = 8[k_B T]$. The dashed line is the prediction of Bhatia and Russel’s original theory, including the error, and the solid line corresponds to this theory corrected by including the missing integral.

(S1) Virk, P. S. *AIChE J.* **1975**, *21* (4), 625–656.

- (S2) Chatterjee, T.; Nakatani, A. I.; Van Dyk, A. K. *Macromolecules* **2014**, *47*, 1155–1174.
- (S3) Bhatia, S.R.; Russel, W.B. *Macromolecules* **2000**, *33*, 5713–5720.